

Modeling Nanoscale Plasmon-assisted Bubble Nucleation and Applications

Edward P. Furlani^{1,2}, Mark T. Swihart², Natalia Litchinitser¹,
Christopher N. Delametter³ and Melissa Carter⁴

Dept. of Electrical Engineering¹, Dept. Chemical & Biological Engineering²,
University at Buffalo (SUNY), Buffalo, NY 14260-4200, efurlani@buffalo.edu

Consumer Digital Imaging Group, Eastman Kodak Company³,
Rochester, New York 14650-2100

Flow Science Inc.⁴, Santa Fe, New Mexico 87505

ABSTRACT

We present a theoretical study of photothermal effects produced by laser illuminated subwavelength metallic nanostructures in a fluid. Such structures exhibit a plasmon resonance at optical wavelengths that enables enhanced conversion of optical to thermal energy. We demonstrate that the photothermal coupling can be tuned to achieve controlled homogeneous bubble generation at the nanoscale. We discuss methods for modeling this phenomenon and fundamental features of the bubble dynamics. We also discuss applications that include therapeutic destruction of tissue at the cellular level and the controlled generation of femtoliter-sized droplets.

Keywords: photothermal analysis, nanoscale bubble nucleation, plasmon-assisted bubble generation, photothermal therapy, plasmonics.

1 INTRODUCTION

Over the last few years there has been growing interest in nanoscale photothermal phenomena associated with the interaction of laser light with subwavelength metallic (e.g. Au and Ag) nanoparticles [1-6]. The conduction electrons in such particles can be resonantly excited at their plasmonic frequencies and the coherent oscillation of the electrons at resonance results in intense absorption and scattering of light and highly localized field enhancement. This unique optical response of subwavelength metallic nanoparticles can be used to achieve controlled and highly localized photothermal energy conversion. This phenomenon has been adapted for use in a wide range of applications, especially diagnostic and therapeutic biomedical applications. In this presentation we model the photothermal process and discuss various applications.

The response of metallic nanoparticles to laser illumination and the resulting thermal effects depend on many factors including the optical absorbance cross-section

of the particle, the intensity and pulse duration of the laser and mechanisms of heat transfer to the surrounding fluid. Aside from the primary effect of heating the particle itself, secondary effects include diffusion of heat into the surrounding fluid and vapor bubble nucleation, if the temperature at the surface of the particle exceeds the vaporization threshold of the fluid. While considerable research has been conducted to understand the optical absorption of plasmonic nanoparticles and thermal

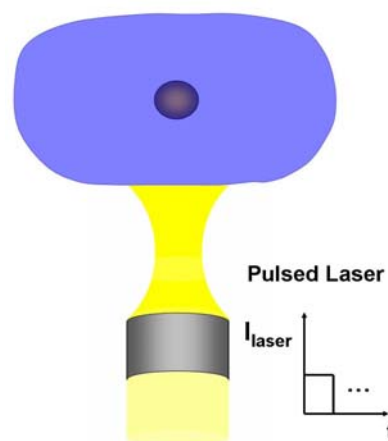


Figure 1: Illustration of pulsed laser illumination of a gold nanoparticle in fluid:

diffusion around them, relatively few studies have focused on the details of the plasmon-assisted bubble nucleation. Experiments have shown that the parameters that govern this process can be tuned to control the size, duration and number of bubbles generated [5].

In this presentation we model and discuss the dynamics of laser-induced bubble generation around metallic nanoparticles in fluid. A rigorous study of this phenomenon requires a coupled electromagnetic-fluidic analysis to predict the simultaneous absorption of incident laser energy, and thermal effects as this energy is transferred from the particle to the surrounding fluid. We simplify the analysis by uncoupling these phenomena. Specifically, we use computational electromagnetics to predict the laser-induced energy absorbed by a gold nanoparticle in fluid taking into account its wavelength dependent optical properties. We identify an optimum wavelength for heating and determine the time-averaged power absorbed by the particle for a given incident laser intensity. The absorbed power predicted from the EM analysis is used as an input to a computational fluid dynamics (CFD) model where it becomes the power generated by the particle, i.e. a heat source for the fluid. The CFD analysis predicts the thermal diffusion from the particle into the surrounding fluid and takes into account homogeneous bubble nucleation once the fluid reaches its superheat temperature. We use CFD to study the nucleation, growth and collapse of a nanobubble around the particle as a function of the intensity and duration of the laser pulse. We discuss aspects of the modeling and various applications.

2 MODELING AND RESULTS

We first consider photothermal bubble generation for an illuminated gold nanoparticle in water (Fig. 1). The particle is 60 nm in diameter and we start with a fullwave EM analysis to determine the optical power absorbed by the particle as a function of the incident wavelength.

2.1 Electromagnetic Analysis

We compute the EM response of the particle under illumination over a range of incident free-space wavelengths: $\lambda = 450\text{-}650\text{nm}$, which span the plasmon resonance wavelength λ_p of the particle in free-space ($\lambda_p \sim 520\text{nm}$). Note that the wavelength of the incident field is shorter in water $\lambda_{\text{H}_2\text{O}} = \lambda/n_{\text{H}_2\text{O}}$ where $n_{\text{H}_2\text{O}} = 1.33$. We solve the time-harmonic equation for the E field

$$\nabla \times (\mu_r^{-1} \nabla \times \mathbf{E}) - k_0^2 \left(\epsilon_r - j \frac{\sigma}{\omega \epsilon_0} \right) \mathbf{E} = 0 \quad (1)$$

using the Comsol finite element-based RF solver. Here, μ_r and ϵ_r are the relative permeability and the complex-valued frequency-dependent permittivity, respectively. The computational domain for the EM analysis is shown in Fig. 2. It spans 1000 nm in the direction of propagation (z-axis), and 250 nm in both the x and y directions. The 60 nm nanoparticle is centered at the origin. Perfectly matched layers (PMLs) are applied at the top and bottom of the

computational domain to reduce backscatter from these boundaries. The PMLs are 100 nm in height, which leaves 800 nm of physical domain along the z-axis, which is labeled. Perfect electric conductor (PEC) (symmetry) conditions are applied at the boundaries perpendicular to the E field at $x = \pm 125$ nm, and perfect magnetic conductor (PMC) (symmetry) conditions at the boundaries perpendicular to the H field at $y = \pm 125$ nm. These symmetry boundary conditions ensure normal incidence of

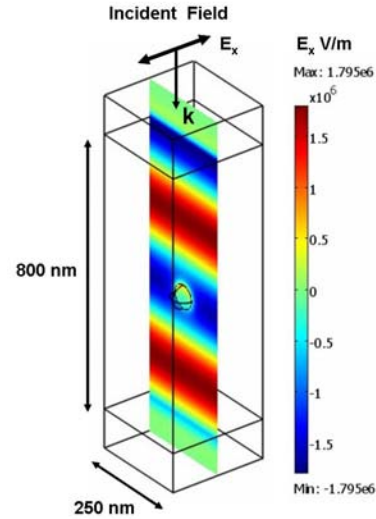


Figure 2: Electromagnetic analysis of an illuminated 60nm gold nanoparticle in fluid. The computational domain and a plot of the E field at $\lambda = 540$ nm (free-space wavelength) are shown.

the respective fields at the boundaries transverse to the direction of propagation, and therefore mimic a 2D array of identical nanoparticles with a center-to-center lattice spacing of 250 nm in both the x and y directions. These boundary conditions simplify the analysis and the lattice distance is chosen to be great enough so that the resulting predictions will reflect the response of the single particle, i.e. there will be negligible coupling with neighboring particles.

The particle is illuminated with a downward directed uniform TEM plane wave with the E field parallel to the x-axis (Fig. 2). The incident field is generated by a time-harmonic surface current source (not shown) positioned in the x-y plane 400 nm above the center of the nanoparticle, immediately below the upper PML as discussed in [7-8]. The magnitude of the surface current is chosen to provide a plane wave in the fluid with a peak amplitude of $E_x = 2 \times 10^6$ V/m (in the absence of the particle). Thus, the irradiance of the of the incident light,

$$I_{inc} = \frac{c \epsilon_0 n_{\text{H}_2\text{O}}}{2} |E_{inc}|^2 \quad (2)$$

is $I_{inc} = 7\text{mW}/\mu\text{m}^2$. We computed the time-averaged power absorbed by the nanoparticle using both the numerical model above and an analytical analysis that is based on the assumption of Rayleigh scattering i.e.

$$Q_{abs} = k\text{Im}g(\alpha)I_{inc} \quad (3)$$

where $k = 2\pi n_{\text{H}_2\text{O}}/\lambda$ and α is the complex-valued polarizability of the particle. We obtained good agreement between these methods as shown in Fig. 3. The analytical analysis yields a somewhat lower and narrower absorption profile because it is based on a dipole approximation, whereas the numerical model takes into account absorption and scattering due to higher order multipole terms. An important consideration in laser heating of metallic nanoparticles is to avoid exceeding the melting or even vaporization temperature of the metal. For gold, these values are $T_m = 1336\text{ K}$ and $T_v = 2933\text{ K}$, respectively. We use the EM analysis described above to determine the laser

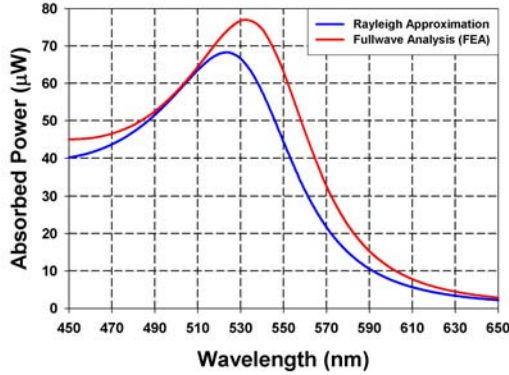


Figure 3: Power absorbed by a 60 nm Au NP in H_2O as a function of λ for $I_{inc} = 7\text{mW}/\mu\text{m}^2$: comparison of numerical and analytical predictions.

irradiance needed to effect bubble nucleation, which is based on fluidic analysis as described in the following.

2.2 Fluidic Analysis

We used CFD analysis to study heat transfer, vaporization and bubble dynamics around an illuminated Au nanoparticle. The volume of fluid (VOF) method as implemented in the FLOW-3D software was used for this analysis [8]. The phase change that initiates homogeneous bubble nucleation occurs when the fluid reaches its superheat temperature, which is $T = 580\text{K}$ for H_2O . The Clausius-Clapeyron equation is used to determine the saturation vapor pressure as a function of temperature, and the rate of change of mass between the fluid and vapor phase is taken to be proportional to the deviation of the fluid from its saturation conditions. The mass flux leaving the liquid surface leads to an increase in pressure within the vapor region causing it to expand as the vapor-liquid

interface moves outward. The vapor region evolves into a bubble. Once formed, the bubble is governed by the ideal gas equation.

We studied an isolated Au nanoparticle in a fluid reservoir. A parametric analysis was initially performed to determine the power and pulse duration required to achieve controlled bubble nucleation without exceeding the melting temperature of the particle (1336K). For the 60 nm particle, an adequate power was found to be $151\ \mu\text{W}$ with a heat pulse duration of 5.2 ns. From the EM analysis (Fig. 3) we find that a laser operating at $\lambda = 532\text{ nm}$ with an irradiance of $I_{inc} = 14\text{mW}/\mu\text{m}^2$ would be sufficient to generate the bubble. The fluidic analysis at this power and pulse duration is shown in Fig. 4. This plot shows the temperature of the nanoparticle during and after the heat pulse and there are inset images that show the generation and collapse of a primary bubble followed by a secondary bubble. Note that during the first 4 us, the temperature of the particle gradually increases from ambient 300K to the superheat temperature 580K at which point a bubble is generated. Once this occurs the particle is surrounded by vapor with a low thermal conductivity and the temperature of the particle increases rapidly to a peak of approximately 1220K, which occurs at the end of the heat pulse. The bubble eventually collapses, bringing fluid back in contact with the particle,

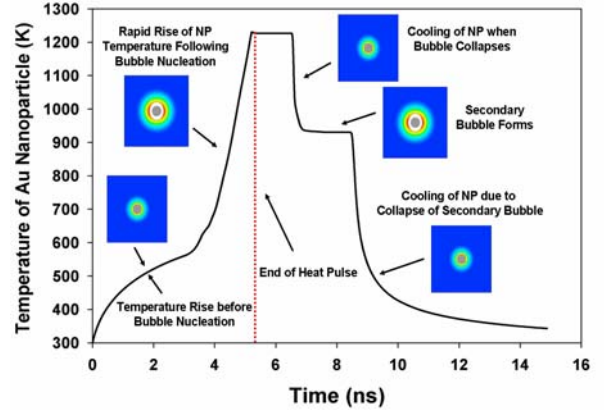


Figure 4: Laser-pulsed 60 nm Au nanoparticle (NP) in H_2O : heating and cooling cycle of a NP showing the particle temperature vs. time with inset images that show the growth and collapse of a primary bubble followed by a secondary bubble.

which cools it from its peak temperature to approximately 950K. At that point, the fluid temperature once again reaches the superheat temperature and a secondary bubble is generated. This process repeats itself when the second bubble collapses and finally cools the particle towards the ambient temperature. We performed additional parametric analysis and found that the number of bubbles generated and their dynamics can be controlled by tuning the power and duration of the heat pulse.

We applied the analysis above to study the viability of a novel optically-activated droplet ejector concept shown in Fig. 5. In this device, a gold nanodisk is positioned beneath an orifice and heated using a pulsed laser. For our proof-of-concept analysis, we chose a disk that is $1.5\ \mu\text{m}$ in diameter and $200\ \text{nm}$ in height. The disk is positioned $0.3\ \mu\text{m}$ beneath an orifice that is $1.2\ \mu\text{m}$ in diameter. The disk is illuminated using a pulsed-laser. The idea is that the laser heats the disk sufficiently to nucleate a bubble, which expands with sufficient pressure to eject a droplet through the orifice. We performed parametric CFD analysis to determine the power and pulse duration required to eject a droplet. We found that a $16.2\ \text{mW}$ heat pulse lasting for $60\ \text{ns}$ is sufficient for drop ejection. We performed a parametric EM analysis to determine the beam irradiance needed to induce the required ejection power. This depends on the optical absorption of the disk, which is a function of wavelength. We computed the power absorbed by the disk for a given irradiance over a range of wavelengths $400\text{-}1000\ \text{nm}$ and found that maximum power was absorbed at $\lambda = 430\text{nm}$. This wavelength does not correspond to a plasmon resonance, but rather to a local maximum in the imaginary part of the permittivity of gold, which governs EM absorption. From the absorption analysis and the known required power, we determined that a beam irradiance of $12\text{mW}/\mu\text{m}^2$ is need for drop ejection. The ejection sequence at the specified power level is shown in Fig. 6. The volume of the ejected droplet is 0.36 femtoliter and it has a velocity of approximately $0.5\ \text{m/s}$.

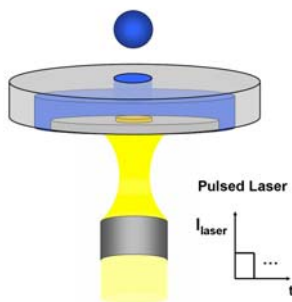


Figure 5: Optically activated droplet ejector: laser illuminated gold nanodisk beneath an orifice.

Significantly, the ejection-refill cycle for this ejector is approximately $1\ \mu\text{s}$, which would enable $1,000,000$ drops to be ejected from a single orifice per second. By comparison, modern thermal bubble-jet ejectors, which are based on electrically-pulsed resistive heating, typically produce picoliter-sized droplets at repetition rates limited to 10s of kilohertz. While many critical fabrication and performance issues remain to be considered, our analysis indicates that photothermal-based drop ejectors could hold potential for a disruptive advance in this field.

3 CONCLUSIONS

Applications of nanoscale photothermal phenomena involving laser illuminated metallic nanoparticles are growing rapidly across various and diverse emerging fields. Progress in this area can be accelerated using multidisciplinary electromagnetic-fluidic modeling, which enables fundamental understanding of underlying processes, and design capability that can be leveraged for determining proof-of-concept and performance optimization. In this presentation, we have demonstrated

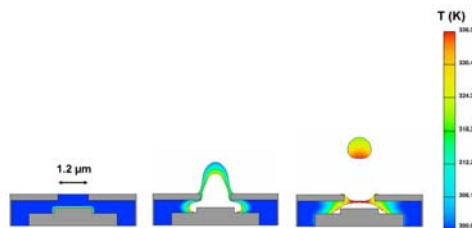


Figure 6: CFD analysis of droplet ejection for laser-pulsed Au nanodisk in H_2O .

the application of such modeling to study both bubble dynamics around a metallic sphere in fluid and a novel optically-activated droplet ejector.

REFERENCES

- [1] Y. Hleb, J. H. Hafner, J. N. Myers, E. Y. Hanna, and D. O. Lapotko, "LANTCET: elimination of solid tumor cells with photothermal bubbles generated around clusters of gold nanoparticles," *Nanomedicine* **3**, 648-667, 2008.
- [2] O. Govorov and H. H. Richardson, "Generating heat with metal nanoparticles," *Nano. Today* **1**, 30-38, 2007.
- [3] Y. Seol, A. Carpenter, and T. Perkins, "Gold nanoparticles: enhanced optical trapping and sensitivity coupled with significant heating," *Opt. Lett.* **31**, 2429-2431, 2006.
- [4] M. Pitsillides, E. K. Joe, X. Wei, R. R Anderson, and C. P. Lin, "Selective cell targeting with light absorbing microparticles and nanoparticles," *Biophys. J.* **84**, 4023-4032, 2003.
- [5] D. Lapotko, Plasmonic nanoparticle-generated photothermal bubbles and their biomedical applications. *Nanomedicine* **7**, 813-845, 2009.
- [6] D. Lapotko, Optical excitation and detection of vapor bubbles around plasmonic nanoparticles. *Opt. Express.*, **17** (4), 2538-2556, 2009.
- [7] E. P. Furlani and A. Baev, "Optical Nanotrapping using Cloaking Metamaterial," *Phys. Rev. E*, **79**, 026607, 2009.
- [8] E. P. Furlani and A. Baev, "Free-space Excitation of Resonant Cavities formed from Cloaking Metamaterial," *J. Mod. Opt.* **56**, 4 523-529, 2009.
- [9] Flow Science Corp. www.flow3D.com.